Spectral and Electrochemical Study of Coordination Molecules $Cu_4OX_6L_4$: $Cu_4OBr_nCl_{(6-n)}(Pyridine)_4$ Complexes

G. ONDREJOVIČ and A. KOTOČOVÁ

Department of Inorganic Chemistry, Faculty of Chemical and Food Technology, Slovak University of Technology, SK-812 37 Bratislava
e-mail: gregor.ondrejovic@stuba.sk

Received 24 February 2004

The tetranuclear $Cu_4OBr_nCl_{(6-n)}(py)_4$ complexes, where py = pyridine and n = 0—6, with trigonal bipyramidal coordination of copper were prepared and their electronic spectra and cyclic voltammograms in nitromethane solutions were measured. The energy, intensity, and half-width of the two overlapped d—d bands were obtained by the Gaussian resolution. The maxima of the high-energy bands assigned to $e(d_{xz}, d_{yz}) \rightarrow a_1(d_{z^2})$ transitions are in a linear correlation with the number of bromoligands, n, $\tilde{\nu}_{2\max}(\mathrm{G})/\mathrm{cm}^{-1} = -53.0n + 13420$. The maxima of the low-energy bands assigned to $e(d_{x^2-y^2}, d_{xy}) \rightarrow a_1(d_{z^2})$ transitions approximate a polynomial correlation $\tilde{\nu}_{1\max}(\mathrm{G})/\mathrm{cm}^{-1} = -7n - 3n^2 + 11300$. Formal reduction potentials $E'_{1/2}$ of the complexes varied with the number of bromoligands in the range 457 mV—519 mV. This variation is described by the equation $E'_{1/2}(n) = E'_{1/2}(3) - k \log[(6-n)/n]$, k represents the constant, its average value is 9.8 mV. The electrochemical results correspond with the electronic spectra suggesting that the electron enters the half-filled d_{z^2} orbital of the copper(II) atom.

Crystal and molecular structure determinations of over 40 $Cu_4OX_6L_4$ complex molecules [1] showed that these molecules consist of three penetrating polyhedra: a coordination tetrahedron OCu_4, a noncoordination octahedron OX_6, and four coordination trigonal bipyramids $CuOX_3L$ (Fig. 1). Bromo- and chloroligands X are bridging, each connecting a pair of copper(II) atoms and at the same time occupying equatorial sites of the trigonal bipyramidal coordination. Outer axial sites of each of the four trigonal bipyramids are occupied by terminal ligands L, which rise out of the molecule in tetrahedral directions. The terminal ligands L are represented by a number of O-, S-, N-, P-, As-, and Sb-donor ligands with different electronic properties, which significantly affect the electronic system of the $Cu_4OX_6L_4$ molecules. Easy electron density transfer between the bonded atoms protects the molecules against redox decomposition [2].

Both, bridging halide ligands X and terminal ligands L may originate inner- and intermolecular interactions. They produce more or less extensive structural distortions, which are well compensated by the molecule as a whole [3].

The $Cu_4OX_6L_4$ molecules can be regarded as coordination supermolecules with a variety of combined polyhedra involving bonding and nonbonding interactions in solids and solutions as well. The properties of these molecules are easily tuned electronically and stereochemically. We decided to investigate spectral and electrochemical properties of the $Cu_4OX_6L_4$ molecules based on fine-tuning by variation of bridging halide ligands X and substituted pyridine and imidazole ligands L. In this introductory paper a complete series of the $Cu_4OBr_nCl_{(6-n)}(py)_4$ molecules is prepared and studied. The results of spectral and voltammetric measurements are presented and the effects of bromide and chloride ligands variation on the spectral and redox properties are discussed.

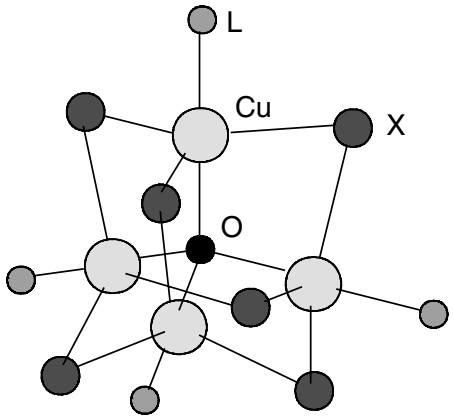

Fig. 1. Structure of $Cu_4OX_6L_4$ molecules.

EXPERIMENTAL

All chemicals used in the synthesis of the complexes were anhydrous and were prepared by standard

procedures. Nitromethane was dried over anhydrous $CaCl_2$ and then twice fractionally distilled. Solution measurements were performed immediately after synthesis of the complexes.

Infrared spectra were recorded with Nicolet Magna 750 spectrophotometer in Nujol mull. Electronic absorption spectra were recorded in Nujol mull and nitromethane solutions with Specord 200 and Nicolet Magna 750 spectrophotometers and processed with Aspect Plus and Microcal Origin 50 software. The Gaussian analysis was performed by means of the zero line subtraction method.

Electrochemical measurements were made on a polarographic analyzer (ECA^{pol} model 110), utilizing three-electrode geometry consisting of a platinum-wire working electrode, a platinum-foil auxiliary electrode, and an aqueous saturated calomel reference electrode (SCE). The SCE was separated from the studied solution by a bridge with a glass of low porosity filled with the nitromethane and the tetrabutylammonium hexafluorophosphate ($[NBu_4][PF_6]$) supporting electrolyte. Cyclic voltammograms of the complexes were measured in nitromethane solution (0.1 mol dm^{-3} $[NBu_4][PF_6]$) under an argon atmosphere at room temperature with scan rates ranging from 20 mV s^{-1} to 500 mV s^{-1}. All potentials were measured with respect to an SCE. The ferrocene/ferrocenium couple was not used as an internal standard for a reactivity of the ferrocene (Fc) with the studied complexes ($E'_{1/2}(Fc/Fc^+) = 0.30$ V *vs.* SCE) in the nitromethane solution. Nitromethane solutions for electrochemical measurements were monitored by electronic spectra, especially by Gaussian resolution of *d*—*d* bands.

Complexes

The methanolato complexes were synthesized by refluxing CuO (0.1 g; 1.26 mmol) with precise stoichiometric amounts of $CuCl_2$ and $CuBr_2$ for 90 min in methanol (15 cm^3). The reaction well proceeds with a slight excess of CuO. Unreacted CuO was filtered off and to methanolic solutions of the $Cu_4OBr_nCl_{(6-n)}(MeOH)_4$ complexes the required amounts of pyridine, each in methanol (5 cm^3), were slowly added under stirring. If pyridine was added in excess, complexes were usually contaminated by other crystalline compounds. Pure microcrystalline products of the $Cu_4OBr_nCl_{(6-n)}(py)_4$ complexes were collected, twice washed with methanol and dried standing on air. Dry solid $Cu_4OBr_nCl_{(6-n)}(py)_4$ complexes were stable for several months. The methanolic solutions of the complexes were protected against moisture.

$Cu_4OCl_6(py)_4$. For $Cu_4OCl_6C_{20}H_{20}N_4$ (M_r = 799.30) w_i(calc.): 31.80 % Cu, 26.61 % Cl, 30.05 % C, 2.52 % H, 7.01 % N; w_i(found): 31.26 % Cu, 26.77 % Cl, 30.82 % C, 2.78 % H, 7.35 % N. Infrared spectra, $\tilde{\nu}/cm^{-1}$: 591 sh, 580 s, 573 sh $\nu(Cu_4O)$, 1606 s, 1576 w, 1491 s, 1450 s (pyridine ring stretching vibrations). Electronic spectra, $\tilde{\nu}_{max}/cm^{-1}$: 13210, 11690 (*d*—*d* bands).

$Cu_4OBrCl_5(py)_4$. For $Cu_4OBrCl_5C_{20}H_{20}N_4$ (M_r = 843.75) w_i(calc.): 30.12 % Cu, 9.47 % Br, 21.01 % Cl, 28.47 % C, 2.39 % H, 6.64 % N; w_i(found): 29.80 % Cu, 10.08 % Br, 19.47 % Cl, 29.10 % C, 2.66 % H, 6.85 % N. Infrared spectra, $\tilde{\nu}/cm^{-1}$: 571 s $\nu(Cu_4O)$, 1606, 1574 w, 1487 s, 1448 s (pyridine ring stretching vibrations). Electronic spectra, $\tilde{\nu}_{max}/cm^{-1}$: 13160, 11640 (*d*—*d* bands).

$Cu_4OBr_2Cl_4(py)_4$. For $Cu_4OBr_2Cl_4C_{20}H_{20}N_4$ (M_r = 888.20) w_i(calc.): 28.62 % Cu, 17.99 % Br, 15.97 % Cl, 27.05 % C, 2.27 % H, 6.31 % N; w_i(found): 27.82 % Cu, 17.98 % Br, 15.95 % Cl, 27.38 % C, 2.13 % H, 6.12 % N. Infrared spectra, $\tilde{\nu}/cm^{-1}$: 561 s $\nu(Cu_4O)$, 1607 s, 1574 w, 1487 s, 1448 s (pyridine ring stretching vibrations). Electronic spectra, $\tilde{\nu}_{max}/cm^{-1}$: 12990, 11550 (*d*—*d* bands).

$Cu_4OBr_3Cl_3(py)_4$. For $Cu_4OBr_3Cl_3C_{20}H_{20}N_4$ (M_r = 932.66) w_i(calc.): 27.25 % Cu, 25.70 % Br, 11.40 % Cl, 25.76 % C, 2.16 % H, 6.01 % N; w_i(found): 27.44 % Cu, 25.60 % Br, 11.24 % Cl, 26.00 % C, 2.05 % H, 5.85 % N. Infrared spectra, $\tilde{\nu}/cm^{-1}$: 554 s $\nu(Cu_4O)$, 1607 s, 1574 w, 1486 s, 1448 s (pyridine ring stretching vibrations). Electronic spectra, $\tilde{\nu}_{max}/cm^{-1}$: 12840, 11510 (*d*—*d* bands).

$Cu_4OBr_4Cl_2(py)_4$. For $Cu_4OBr_4Cl_2C_{20}H_{20}N_4$ (M_r = 977.11) w_i(calc.): 26.01 % Cu, 32.71 % Br, 7.26 % Cl, 24.58 % C, 2.06 % H, 5.73 % N; w_i(found): 24.95 % Cu, 32.78 % Br, 7.39 % Cl, 25.02 % C, 1.98 % H, 5.55 % N. Infrared spectra, $\tilde{\nu}/cm^{-1}$: 547 s $\nu(Cu_4O)$, 1607 s, 1574 w, 1486 s, 1447 s (pyridine ring stretching vibrations). Electronic spectra, $\tilde{\nu}_{max}/cm^{-1}$: 12740 sh, 11470 (*d*—*d* bands).

$Cu_4OBr_5Cl(py)_4$. For $Cu_4OBr_5ClC_{20}H_{20}N_4$ (M_r = 1021.56) w_i(calc.): 24.88 % Cu, 39.11 % Br, 3.47 % Cl, 23.52 % C, 1.97 % H, 5.48 % N; w_i(found): 23.88 % Cu, 38.70 % Br, 3.03 % Cl, 22.76 % C, 1.90 % H, 5.30 % N. Infrared spectra, $\tilde{\nu}/cm^{-1}$: 540 s $\nu(Cu_4O)$, 1607 s, 1574 w, 1486 s, 1447 s (pyridine ring stretching vibrations). Electronic spectra, $\tilde{\nu}_{max}/cm^{-1}$: 12720 sh, 11440 (*d*—*d* bands).

$Cu_4OBr_6(py)_4$. For $Cu_4OBr_6C_{20}H_{20}N_4$ (M_r = 1066.01) w_i(calc.): 23.84 % Cu, 44.97 % Br, 22.53 % C, 1.89 % H, 5.26 % N; w_i(found): 24.42 % Cu, 44.79 % Br, 23.12 % C, 2.01 % H, 5.35 % N. Infrared spectra, $\tilde{\nu}/cm^{-1}$: 534 s $\nu(Cu_4O)$, 1606 s, 1574 w, 1487 s, 1446 s (pyridine ring stretching vibrations). Electronic spectra, $\tilde{\nu}_{max}/cm^{-1}$: 12700 sh, 11390 (*d*—*d* bands).

RESULTS AND DISCUSSION

The $Cu_4OBr_nCl_{(6-n)}(py)_4$ complexes, n = 0—6, were prepared by reaction of pyridine with $Cu_4OBr_nCl_{(6-n)}(MeOH)_4$ complexes in methanolic solutions. The Cu_4O vibration of the molecules of synthesized

complexes is affected by the variation of the bridging bromide and chloride ligands. The Cu_4O band maxima occur between 534 cm^{-1} and 580 cm^{-1} for hexabromo and hexachloro molecules, respectively. The corresponding Cu_4O bands practically do not differ from those previously reported for the molecules with $n = 0$, 6 [4] and $n = 3$ [5].

The fine-tuning of the Cu_4O vibration by halide ligands can be described by a characteristic linear correlation [6] between the wavenumbers of the Cu_4O bands $\tilde{\nu}(Cu_4O)$ and the number of bromide ligands n ($R^2 = 0.9928$)

$$\tilde{\nu}(Cu_4O)/cm^{-1} = -7.60n + 578 \qquad (1)$$

The linear fine-tuning (*1*) is associated with increasing Cu—O bond lengths from minimum 188(2) pm for $Cu_4OCl_6(py)_4$ [7] to maximum 193(1) pm for $Cu_4OBr_6(py)_4$ [8], and thus, with the size of the OCu_4 tetrahedron. Such enlargement of the OCu_4 tetrahedron in structurally similar $Cu_4OBr_nCl_{(6-n)}(OPPh_3)_4$ complexes [3] corresponds to the increasing value of the cubic lattice parameter computed from diffraction patterns. The distinct linear correlation between the lattice parameter and the $\tilde{\nu}(Cu_4O)$ wavenumbers reflects the increasing volume of the Cu_4OX_6 structural unit with the increasing number of bromoligands. The crystal and molecular structure of the $Cu_4OBr_3Cl_3(OPPh_3)_4$ complex showed that the bridging positions are occupied by chloride and bromide ligands statistically in the ratio 0.5 : 0.5 with the Cu—X bond length 246.1(2) pm [3].

The pyridine Cu—N distances vary from minimum 194(2) pm for $Cu_4OCl_6(py)_4$ [7] to maximum 207(2) pm [8] for $Cu_4OBr_6(py)_4$ molecules. This is due, presumably, to the increase in the size of the molecule upon replacement of chloroligands by bromoligands, pushing the pyridine rings further out. The longer Cu—N distances allow the bromoligands on the corresponding tetrahedral faces in adjacent molecules to interact with each other [8]. Although the coordination OCu_4 tetrahedra in the $Cu_4OCl_6(py)_4$ molecules are regular, the noncoordination OCl_6 octahedra deviate quite markedly from regularity. These deviations are associated with the variations in the Cu—Cl distances and especially in the Cl—Cu—Cl angles (108°—138°), but not in the Cu—Cl—Cu angles (79°—81°). There is no relationship between the distortion of the OCl_6 octahedra and the intramolecular interatomic contact [7]. The only intermolecular contacts between adjacent hexachloro molecules are either pyridine ring—pyridine ring contacts or pyridine ring—chloride ligands contacts. The intermolecular changes and distortions occur in an ordered fashion and are transmitted from a given molecule to its neighbours.

The temperature variation of the effective magnetic moment, μ_{eff}, for $Cu_4OX_6L_4$ complexes has been classified into three classes [9]. Both $Cu_4OCl_6(py)_4$ and $Cu_4OBr_6(py)_4$ complexes are antiferromagnetic in nature and have been arranged into class II compounds as those with relatively weak crystal field along the three-fold axis in C_{3v} symmetry of copper(II) atoms.

The copper(II) atoms in the $Cu_4OCl_6(py)_4$ and $Cu_4OBr_6(py)_4$ molecules occur in considerably compressed trigonal bipyramids with relatively short axial Cu—N and Cu—O bonds and much longer equatorial Cu—X bonds. The pyridine and oxygen ligands generate a strong axial ligand field, while halide ligands in the equatorial positions are known as ligands producing weak ligand fields. For such a case the suggested one-electron ground state copper configuration is $a_1(d_{z^2}) > e(d_{xy} \approx d_{x^2-y^2}) > e(d_{xz} \approx d_{yz})$ [10].

The electronic spectra of solid $Cu_4OBr_nCl_{(6-n)}(py)_4$ complexes show two overlapping d—d bands, ν_1 and ν_2 attributed to ${}^2E^{(1)} \leftarrow {}^2A_1'$ and ${}^2E^{(2)} \leftarrow {}^2A_1'$ transitions, respectively, in a trigonal bipyramidal ligand field with C_{3v} symmetry [5]. The position of the ν_1 and ν_2 bands in the electronic spectra of solid $Cu_4OBr_nCl_{(6-n)}(py)_4$ molecules results from a cooperation of two main tendencies, the ligand field strength and the Cu—N, Cu—O, and Cu—X bond lengths. The ligand field strength increases with the number of chloride ligands since these ligands have in the complex molecules higher ionization energy than the bromide ligands. More bulky bromide ligands cause the lengthening of the Cu—N and Cu—O bonds. As a consequence, the energy of $a_1(d_{z^2})$ orbital decreases. The Cu—Br bonds are longer than the Cu—Cl bonds and hence, the $e(d_{x^2-y^2}, d_{xy})$ levels tend to have lower energy.

The low-energy bands ν_1 of solids assigned to $e(d_{x^2-y^2}, d_{xy}) \rightarrow a_1(d_{z^2})$ transitions were found as well resolved bands with absorption maxima at 11390 cm^{-1} for hexabromo and 11690 cm^{-1} for hexachloro complex, while high-energy bands ν_2 assigned to $e(d_{xz}, d_{yz}) \rightarrow a_1(d_{z^2})$ transitions were found with maxima between $\approx$ 12700 cm^{-1} and 13210 cm^{-1}, respectively. Absorption maxima of ν_1 bands, $\tilde{\nu}_{1max}$ are fine-tuned by number of bromoligands as indicated by a linear correlation (*2*) ($R^2 = 0.9752$) between absorption maxima, $\tilde{\nu}_{1max}$ and the number of bromide ligands, n

$$\tilde{\nu}_{1max}/cm^{-1} = -49.0n + 11680 \qquad (2)$$

However, ν_2 bands were satisfactorily resolved only for the complexes with $n = 0$—3, but less reliable linear correlation ($R = 0.9260$) has been found due to unresolved bands.

The above presented linear fine-tunings (eqns (*1*) and (*2*)) found for solid $Cu_4OBr_nCl_{(6-n)}(py)_4$ complexes indicate that the coordination (OCu_4 and $CuOX_3L$) and noncoordination (OX_6) distortions originating in the halide ligand variation are gradually

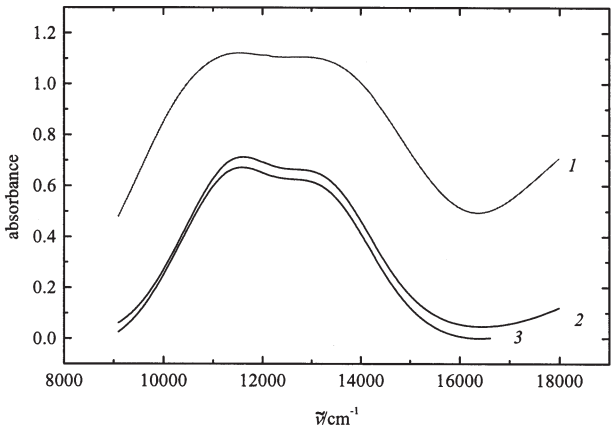

Fig. 2. Bands d—d in the electronic spectra of the $Cu_4OBr_3Cl_3(py)_4$ complex. *1.* Solid in Nujol mull, *2.* nitromethane, *3.* chloroform solutions ($c = 5 \times 10^{-4}$ mol dm^{-3}).

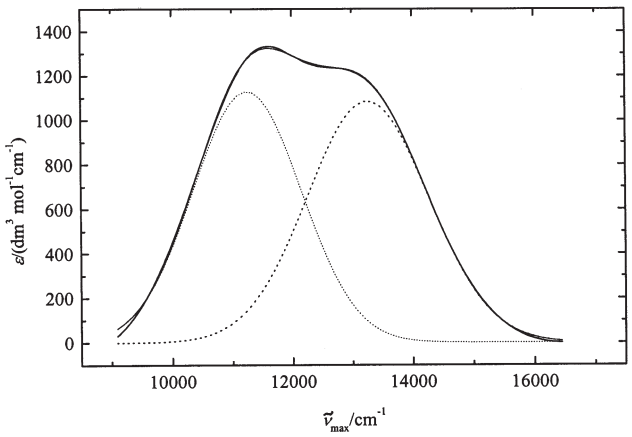

Fig. 3. Typical Gaussian resolution of ν_1 and ν_2 bands for $Cu_4OBr_3Cl_3(py)_4$ molecules in nitromethane.

ordered from molecule to molecule determining the nature of the packing. As a result, the ν_1 and most of ν_2 bands are resolved, with the absorption maxima separations $\tilde{\nu}_{2max} - \tilde{\nu}_{1max} \approx 1300$ cm^{-1} for hexabromo and $\tilde{\nu}_{2max} - \tilde{\nu}_{1max} \approx 1500$ cm^{-1} for hexachloro molecules.

Nitromethane solutions of the $Cu_4OBr_nCl_{(6-n)}(py)_4$ molecules in the concentration range 1.5×10^{-4}—1.5×10^{-3} mol dm^{-3} obey Lambert—Beer's law with respect to both double d—d bands and single ν_1(G) and ν_2(G) bands resolved by Gaussian analysis. The integral Gaussian band intensities are almost linearly reduced (about 10 %) by free pyridine added to the measured solutions of the complexes ($c = 5 \times 10^{-4}$ mol dm^{-3}) up to concentration 3×10^{-3} mol dm^{-3} indicating that the $Cu_4OBr_nCl_{(6-n)}(py)_4$ molecules in nitromethane do not observably dissociate and the solutions are free of other species absorbing in the region of ν_1 and ν_2 bands. The supporting electrolyte $[NBu_4][PF_6]$ ($c = 0.1$ mol dm^{-3}) in nitromethane solutions for electrochemical measurements reduces peak absorbances of ν_1(G) and ν_2(G) bands by about 6 %. The peak maxima of these bands remain practically unaffected.

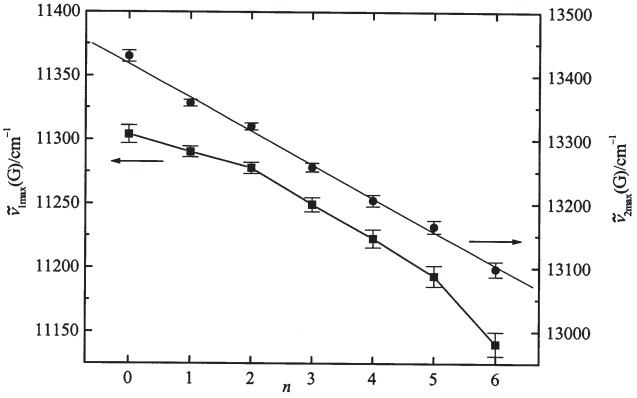

Fig. 4. Correlations between absorption maximum of Gaussian ν_1(G), ν_2(G) bands and the number of bromoligands, n, for $Cu_4OBr_nCl_{(6-n)}(py)_4$ molecules in nitromethane.

Nitromethane solution ν_1 and ν_2 bands are overlapped to a higher extent compared to corresponding bands of solid $Cu_4OBr_nCl_{(6-n)}(py)_4$ spectra (Fig. 2). Simple inspection of the solution electronic spectra showed that ν_1 bands are well resolved, unlike the ν_2 bands, which are represented by shoulders for all of the complexes. The absorption maxima of $\nu_1$bands between approximately 11600 cm^{-1} and 11620 cm^{-1} are practically unaffected by the variation of halide ligands. The ν_2 shoulders move away of "static" ν_1 bands to higher energies of ≈12600 cm^{-1} for hexabromo molecules and ≈ 12900 cm^{-1} for hexachloro molecules. The maxima of ν_1 and ν_2 bands for individual solvated $Cu_4OBr_nCl_{(6-n)}(py)_4$ molecules are close to each other, separated only by ≈ 1000 cm^{-1} for hexabromo and ≈1200 cm^{-1} for hexachloro molecules. Therefore, strongly overlapped ν_1 and ν_2 bands were resolved by Gaussian analysis.

An example of the Gaussian resolution of ν_1 and ν_2 bands for $Cu_4OBr_3Cl_3(py)_4$ molecule is shown in Fig. 3. The results of Gaussian analysis are summarized in Table 1. The correlations between absorption maxima of Gaussian $\tilde{\nu}_{1max}$(G), $\tilde{\nu}_{2max}$(G) bands and the number of bromide ligands in the $Cu_4OBr_nCl_{(6-n)}(py)_4$ molecules are plotted in Fig. 4. While the correlation between $\tilde{\nu}_{2max}$(G) band maxima and the number of bromide ligands, n is linear ($R^2 = 0.9954$)

$$\tilde{\nu}_{2max}(G)/cm^{-1} = -53.0n + 13420 \qquad (3)$$

corresponding curve for $\tilde{\nu}_{1max}$(G) band fits a linear correlation less effectively ($R^2 = 0.97254$)

$$\tilde{\nu}_{1max}(G)/cm^{-1} = -25.0n + 11320 \qquad (4)$$

Table 1. Gaussian Parameters of d—d Bands, Wavenumber $\tilde{\nu}$(G), Half-Width W(G), and Molar Absorption Coefficient ε(G) for $Cu_4OBr_nCl_{(6-n)}(py)_4$ Complexes in Nitromethane

Complex	$\tilde{\nu}_1$(G)	W_1(G)	ε_1(G)	$\tilde{\nu}_2$(G)	W_2(G)	ε_2(G)
	cm^{-1}	cm^{-1}	$dm^3\ mol^{-1}\ cm^{-1}$	cm^{-1}	cm^{-1}	$dm^3\ mol^{-1}\ cm^{-1}$
$Cu_4OCl_6(py)_4$	11300	1950	780	13430	2070	690
$Cu_4OBrCl_5(py)_4$	11290	1860	890	13360	2020	820
$Cu_4OBr_2Cl_4(py)_4$	11280	1840	840	13320	2020	780
$Cu_4OBr_3Cl_3(py)_4$	11250	1800	1130	13260	2010	1080
$Cu_4OBr_4Cl_2(py)_4$	11220	1760	1060	13210	2010	1050
$Cu_4OBr_5Cl(py)_4$	11190	1750	1060	13160	2000	1060
$Cu_4OBr_6(py)_4$	11160	1740	1100	13120	2000	1120

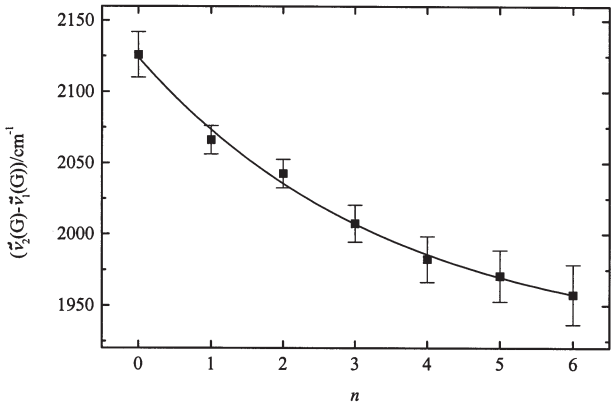

Fig. 5. The correlation between the difference $\tilde{\nu}_{2max}(G) - \tilde{\nu}_{1max}(G)$ and the number of bromoligands, n, for $Cu_4OBr_nCl_{(6-n)}(py)_4$ molecules in nitromethane.

It better approximates a polynomial correlation ($R^2 = 0.99614$).

$$\tilde{\nu}_{1max}(G)/cm^{-1} = -7n - 3n^2 + 11300 \qquad (5)$$

The linear correlation (*3*) associated with $e(d_{xz}, d_{yz}) \rightarrow a_1(d_{z^2})$ transition corresponds to a gradual ligand field weakening in the trigonal plane and the gradual decrease of the d_{z^2} energy levels as a result of the Cu—X, Cu—N, and Cu—O bond lengthenings. The $e(d_{xz}, d_{yz})$ energy levels are practically unaffected by these Cu—ligand bond lengths. The linear variation of the ligand field strength corresponds to a linear correlation between Mulliken group electronegativities of the $Cu_4OBr_nCl_{(6-n)}(py)_4$ molecules and the number of bromoligands n [6]. This consideration may also be applied for ν_1(G) bands associated with $e(d_{x^2-y^2}, d_{xy}) \rightarrow a_1(d_{z^2})$ transition. "Deviations from linearity" may presumably reflect the $e(d_{x^2-y^2}, d_{xy})$ energy levels, which are affected by a considerable Cu—X bond length difference at both ends of the molecular series. Here dominates a great difference in the number of the chloro- and bromoligands present in the same molecule.

A plot of $[\tilde{\nu}_{2max}(G) - \tilde{\nu}_{1max}(G)]$ *vs.* number of bromide ligands, n (Fig. 5) indicates that the $e(d_{x^2-y^2}, d_{xy})$ energy levels tend to approach those of $e(d_{xz}, d_{yz})$, especially for the $Cu_4OBr_nCl_{(6-n)}(py)_4$ molecules containing high number of less electronegative bromide ligands. A fine-tuning of the difference between these energy levels may be described by a first-order exponential decay correlation

$$[\tilde{\nu}_{2max}(G) - \tilde{\nu}_{1max}(G)]/cm^{-1} = 205e^{-n/3.0} + 1900 \qquad (6)$$

Recently, a copper-nickel series of heterobimetallic complexes $[(\mu_4\text{-}O)(N,N\text{-diethylnicotinamide})_4Cu_{4-x}\{Ni(H_2O)\}_xCl_6]$ (x = 0—4) was electrochemically studied in strong coordinating dimethyl sulfoxide solvent (DMSO) [11]. It was observed that DMSO molecules increase the coordination number of each Cu^{II} centre to six changing the geometry of the Cu^{II} centres from distorted trigonal bipyramidal to pseudo-octahedral. These complexes remain intact and tetranuclear in DMSO and contain one denc and one dmso molecules per Cu^{II} as the electroactive species. However, the molecular structure and coordination of the copper(II) atoms in these species are not exactly known and are significantly different from the studied $Cu_4OBr_nCl_{(6-n)}(py)_4$ molecules in nitromethane.

The $Cu_4OBr_nCl_{(6-n)}(py)_4$ molecules, the structure and coordination of which remain intact in non-coordinating nitromethane solvent (supporting electrolyte $[NBu_4][PF_6]$), were electrochemically reduced in the potential range from 0 to 1000 mV.

$$Cu_4OBr_nCl_{(6-n)}(py)_4 + e^- = [Cu_4OBr_nCl_{(6-n)}(py)_4]^- \qquad (7)$$

Each of these reduction steps was quasi-reversible and was observed to change with the number of bromoligands in the $Cu_4OX_6(py)_4$ molecules from 148 mV to 196 mV (Table 2). The cyclic voltammetric curves with single anodic and cathodic peaks shown in Fig. 6 are representative of the voltammetric behaviour of the complexes studied. The cyclic voltammograms were evaluated according to a theory published in the literature [12].

The existence of the charged polynuclear [Cu_4O-

Table 2. Voltammetric Data for $Cu_4OBr_nCl_{(6-n)}(py)_4$ Complexes in Nitromethane at Room Temperature and Scan Rate = 100 mV s^{-1}

Complex	E_{pa}/mV	E_{pc}/mV	$(E_{pa} - E_{pc})$/mV	$E'_{1/2}$/mV	I_{pa}/I_{pc}
$Cu_4OCl_6(py)_4$	531	383	148	457	0.971
$Cu_4OBrCl_5(py)_4$	559	403	156	481	0.981
$Cu_4OBr_2Cl_4(py)_4$	580	384	196	482	0.906
$Cu_4OBr_3Cl_3(py)_4$	570	406	164	488	0.952
$Cu_4OBr_4Cl_2(py)_4$	583	405	178	494	0.971
$Cu_4OBr_5Cl(py)_4$	571	419	152	495	0.997
$Cu_4OBr_6(py)_4$	603	435	168	519	0.980

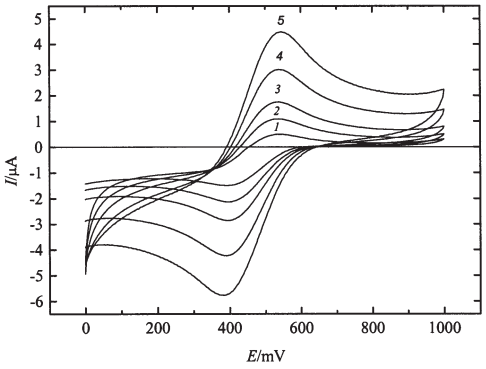

Fig. 6. Typical cyclic voltammogram for $Cu_4OCl_6(py)_4$ complex at different scan rates. *1.* 20 mV s^{-1}, *2.* 50 mV s^{-1}, *3.* 100 mV s^{-1}, *4.* 250 mV s^{-1}, *5.* 500 mV s^{-1}.

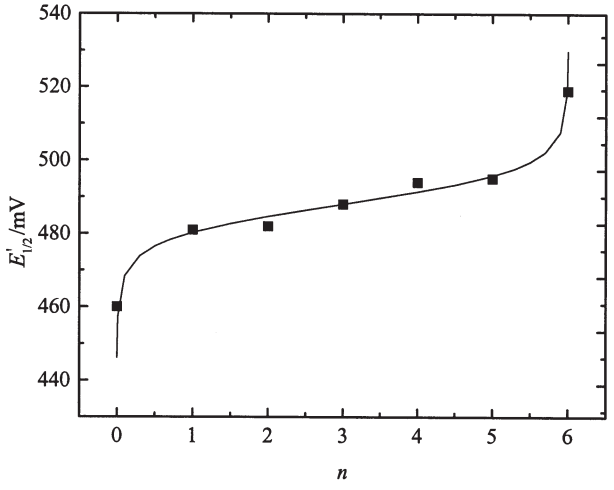

Fig. 7. Dependence of $E'_{1/2}$ *vs.* *n*, scan rate = 100 mV s^{-1}; experimental data (■), calculated data using eqn (*8*) (—).

$Br_nCl_{(6-n)}(py)_4]^-$ molecules in the electrochemical process may be supported by a possible stabilization effect [13] originating in large $[NBu_4]^+$ counter ion, which is supplied by supporting electrolyte. A pentacoordination for the Cu^I (d^{10}) atoms in the polynuclear anionic $[Cu_4OBr_nCl_{(6-n)}(py)_4]^-$ molecules may be preserved. However, generally for the Cu^I (d^{10}) the coordination number four is predominantly found [14]. However, the anionic $[Cu_4OBr_nCl_{(6-n)}(py)_4]^-$ molecules with a higher number of the bromide ligands are less stable and incline to a less reversible reduction process.

The redox properties ($E'_{1/2} = (E_{pa} + E_{pc})/2$) of the studied complexes are changed with the increasing number of bromide ligands from the values 457 mV to 519 mV for hexachloro and hexabromo derivatives, respectively (Fig. 7). This curve can be described by the equation similar to the Nernst one

$$E'_{1/2}(n)/\text{mV} = E'_{1/2}(3) - k \log [(6-n)/n] \qquad (8)$$

where $E'_{1/2}(3)$ is an "internal standard potential", which equals the formal potential, when number of the bromide ligands $n = 3$. The k is a constant, its average value is 9.8 mV. The numerator $(6-n)$ is the number of chloride ligands and the analogy with the Nernst equation is "a concentration of the reducing agent". The denominator, n, the number of bromide ligands is then "a concentration of the oxidizing agent". The $Cu_4OBr_nCl_{(6-n)}(py)_4$ molecular series represents in this way "the solution" with gradually changing the ratio of reduced and oxidized species.

Between electrochemical data and crystal field data, there is usually no useful correlation [15], since the electrode potentials are the differences in ground state energies of Cu^{II}, whereas the spectral properties are differences in the ground state and excited states of Cu^{II}. Nevertheless, the two properties can be correlated in terms of ligand field effects. Plots for $E'_{1/2}$ *vs.* $\tilde{\nu}_{2max}(G)$ presented in Fig. 8 show clear correlations between electrochemical data and *d—d* transitions ($R^2 = 0.9871$).

$$E'_{1/2}/\text{mV} = 487 - 16.7 \log [(13100\ \text{cm}^{-1} - \tilde{\nu}_{2max}(G))/(\tilde{\nu}_{2max}(G) - 13420\ \text{cm}^{-1})] \qquad (9)$$

The key element of these correlations seems to be the energy of the copper(II) half-filled ground state $a_1(d_{z^2})$ orbital. The lower the energy of the $a_1(d_{z^2})$ orbital, the higher the electron affinity of

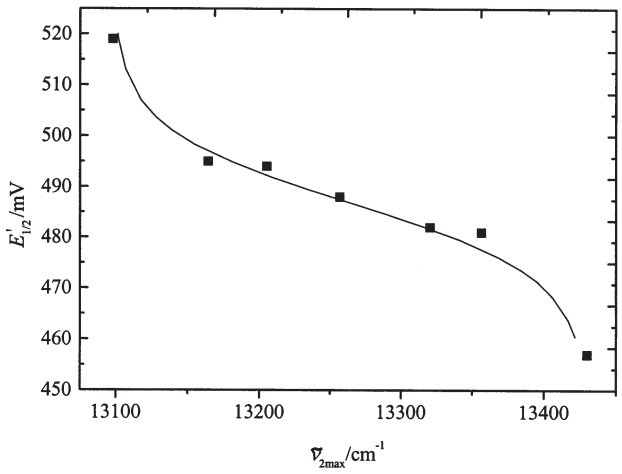

Fig. 8. Dependence of $E'_{1/2}$ *vs.* $\tilde{\nu}_{2\max}$(G), scan rate = 100 mV s^{-1}; experimental data (■), calculated data using eqn (*9*) (—).

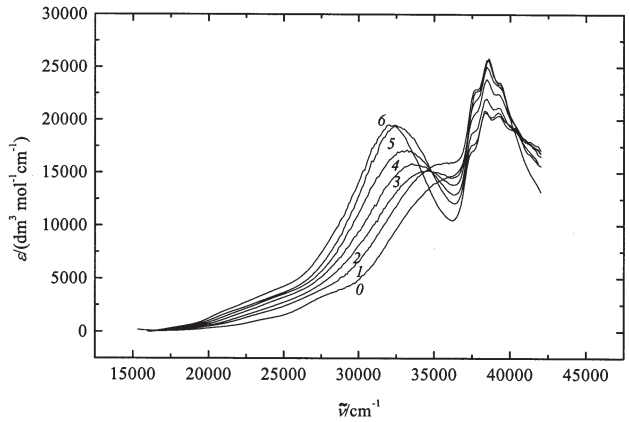

Fig. 9. Charge-transfer spectra of individual $Cu_4OBr_nCl_{(6-n)}(py)_4$ molecules in chloroform.

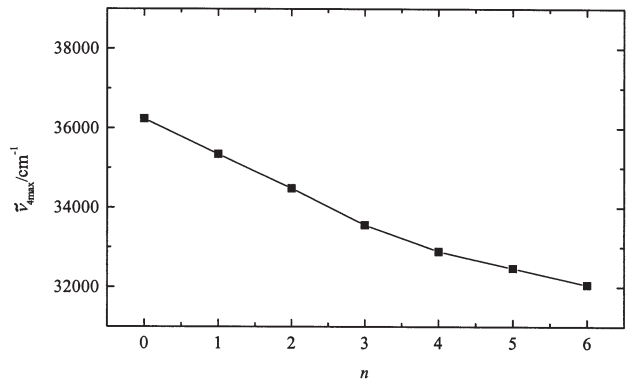

Fig. 10. Dependence of charge-transfer band, $\tilde{\nu}_{4\max}$, on the number of bromoligands, n, for $Cu_4OBr_nCl_{(6-n)}(py)_4$ molecules in chloroform.

the molecules to form corresponding anionic species $[Cu_4OBr_nCl_{(6-n)}(py)_4]^-$ and hence the higher value of $E'_{1/2}$. None of the copper(II) atoms in a single $Cu_4OBr_nCl_{(6-n)}(py)_4$ molecule should be electrochemically preferred for the reduction, since the varied polyhedral halide ligand positions are occupied statistically.

Compared with *d*—*d* transitions better correlations may be anticipated between charge transfer data and differences between appropriate redox couples [15]. The charge transfer region in the electronic spectra of the $Cu_4OBr_nCl_{(6-n)}(py)_4$ molecules in nitromethane is overlapped by nitromethane absorptions themselves.

The $Cu_4OBr_nCl_{(6-n)}(py)_4$ molecules in chloroform exhibit a complex pattern of CT bands as shown in Fig. 9. There is seen an isosbestic-like point at 34660 cm^{-1} indicating an apparent equilibrium among the molecules having mixed-halide coordination (n = 1—5). Relatively narrow halide-independent pattern of CT bands with maxima at about 38500 cm^{-1} may be assigned to pyridine $\pi \rightarrow \pi^*$ and N $\rightarrow$ Cu LMCT transitions. Broad CT absorption bands ν_4 with maxima between 36230 cm^{-1} and 32050 cm^{-1} for hexachloro and hexabromo molecules, respectively, which are strongly halide-dependent (Fig. 9) have been assigned [4] in C_{3v} symmetry to symmetry-allowed halogen-to-copper charge transfer (LMCT) transition $^2E \leftarrow {}^2A_1$. Weak halide-dependent shoulders ν_3 between 28000 cm^{-1} and 24000 cm^{-1} assigned to symmetry-forbidden halide-to-copper CT transitions $^2A_2 \leftarrow {}^2A_1$ cannot be reliably resolved.

The reduction process (*7*) may be related to copper-to-pyridine charge transfer (MLCT) bands $Cu(d_{z^2}) \rightarrow py(\pi^*)$. The energies of these bands should increase with the number of bromide ligands in the $Cu_4OBr_nCl_{(6-n)}(py)_4$ molecules. The bands probably occur as weak shoulders between 28000 cm^{-1} and 20000 cm^{-1}. However, this region is obscured with strong LMCT bands. Due to the CT bands pattern complexity the MLCT bands cannot be identified either by inspection or Gaussian resolution. Nevertheless, energies of LMCT bands ν_4 indirectly indicate that the reduction process (*7*) proceeds since the plot of $\tilde{\nu}_{4\max}$ *vs.* n (Fig. 10) shows decreasing energy of LMCT $X(\sigma) \rightarrow Cu(d_{z^2})$ transition with the number of bromide ligands, n, in the $Cu_4OBr_nCl_{(6-n)}(py)_4$ molecules.

Acknowledgements. We thank the Slovak Grant Agency VEGA for financial support (Grant No. 1/9251/02).

REFERENCES

1. Melník, M., Kabešová, M., Dunaj-Jurčo, M., and Holloway, C. E., *J. Coord. Chem. 41*, 35 (1997).
2. Ondrejovič, G., Valigura, D., Makáňová, D., Koman, M., Kotočová, A., Jorík, V., and Broškovičová, A., *New J. Chem. 21*, 661 (1997).
3. Jorík, V., Koman, M., Makáňová, D., Mikloš, D.,

Broškovičová, A., and Ondrejovič, G., *Polyhedron 15*, 3129 (1996).
4. tom Dieck, H., *Inorg. Chim. Acta 7*, 397 (1973).
5. Brown, D. S., Hopkins, T. G., and Norbury, A. H., *Inorg. Nucl. Lett. 9*, 971 (1973).
6. Ondrejovič, G. and Kotočová, A., *Chem. Pap. 55*, 221 (2001).
7. Kilbourn, B. T. and Dunitz, J. D., *Inorg. Chim. Acta 1*, 209 (1967).
8. Swank, D. D., Nielson, D. O., and Wilett, R. D., *Inorg. Chim. Acta 7*, 91 (1973).
9. Wong, H., tom Dieck, H., O'Connor, C. J., and Sinn, E.*, J. Chem. Soc., Dalton Trans. 1980*, 786.
10. Hathaway, B. J. and Billing, D. E., *Coord. Chem. Rev. 5*, 143 (1970).
11. Workie, B., Dubé, C. E., Aksu, L., Kounaves, S. P., Robat, A., Jr., and Davies, G., *J. Chem. Soc., Dalton Trans. 1997*, 1739.
12. Nicholson, R. S. and Shain, I., *Anal. Chem. 36*, 706 (1964).
13. Basolo, F., *Coord. Chem. Rev. 3*, 213 (1968).
14. Holloway, C. E. and Melník, M., *Rev. Inorg. Chem. 15*, 147 (1995).
15. Lever, A. B. P., *Inorganic Electronic Spectroscopy*, p. 776. Elsevier, Amsterdam, 1984.